Proceedings of the 21st ICSMGE, Vienna, Austria, 14 – 19 June 2026. Pistrol, Adam & Schweiger (eds.)
Published by: ÖGG, Austrian Society for Geomechanics, Salzburg, Austria, ISBN 978-3-9503898-4-5
https://doi.org/10.53243/ICSMGE2026-1774

Estimation of buoyancy factor during inclined lateral breakout of on-bottom pipelines in clay

Abhishek Ghosh Dastider, Namburi Gowtham
Indian Institute of Technology Kharagpur, India, abhishek.dastider@civil.iitkgp.ac.in

Santiram Chatterjee
Indian Institute of Technology Bombay, India

ABSTRACT: The two contributing components for the inclined lateral breakout resistance of an on-bottom pipeline are the geotechnical resistance and the resistance induced by the weight of the displaced soil. This latter resistance component (i.e., the buoyancy effect) becomes more pronounced when the effect of heave formation at the ground surface (during the pipe installation) is included within the calculation. In this research, large deformation finite element (LDFE) analyses were performed to account for the surface heave while estimating lateral breakout resistance of a partially embedded pipe. The soil is assumed to be weightless as well as with self-weight in the LDFE analyses. This exercise aids in precise estimation of the resistance component induced by the weight of the soil. The buoyancy factors (i.e., for vertical and horizontal capacities, f_{bv} and f_{bh}) are estimated by dividing the soil weight-induced resistance component with the weight of the displaced soil. The present research reports buoyancy factors f_{bv} and f_{bh} for pipe movements in various directions, utilizing an existing equation, however including the effect of heave. Moreover, the dimensions of the heave are found to vary with the shear strength gradient of the clay. Consequently, the variation of buoyancy factors for soil with different shear strength gradients is also provided. These buoyancy factors are finally reported in a tabulated form for the use of the readers. Findings from the present research can be useful in precise estimation of breakout resistance of on-bottom pipelines, for their design against controlled buckling.

KEYWORDS: Pipelines, Clay, Breakout resistance, Buoyancy, Shear strength gradient.

1 INTRODUCTION

Deepwater offshore pipelines, often laid directly on soft clayey seabed (without constructing a trench), gains partial embedment due to its own weight and stress concentration during the installation process. During embedment, soil heave usually forms at the ground surface surrounding the pipeline. These pipelines usually operate at a very high temperature and pressure which results in a significantly higher loading compared to the as-laid condition. The axial stress induced due to the temperature change causes the pipe to buckle and eventually breakout from its partially embedded position (Bruton et al. 2005; Dingle et al. 2008, White and Cathie 2011). The heave formed at the time of installation significantly contribute in the lateral resistance experienced by the pipe during thermally-induced buckling (Merifield et al. 2009; Chatterjee et al. 2012 a, b). Stability or controlled movement against this thermal loading are a crucial factor in the design of deepwater pipelines and are heavily dependent on the precise assessment of the mobilized pipe-soil resistance.

Breakout resistance experienced by the pipe while moving in different directions can be divided into two components - geotechnical resistance due to shear strength of the soil and buoyancy effect arising from the weight of the displaced soil. Literature expressed this buoyancy component of the mobilized resistance as a product between weight of displaced soil volume and a buoyancy factor f_b. Researchers quantified f_b against both vertical and horizontal movement of pipe (Randolph and White 2008; Merifield et al. 2009; Chatterjee et al. 2012b; Chatterjee et al. 2014). This factor equals to 1 for a 'wished-in-place' pipe (i.e., where the soil heave formation during the pipe installation process has not been considered) subjected to vertical displacement. Whereas under purely horizontal motion, with gap opening at the rear of the pipe, f_b is equal to 0.5. As the presence of surface heave leads to increase in the work required to penetrate the pipe, the f_b factor enhances (i.e., becomes higher than unity for vertical movement) for the pushed-in-place condition. Merifield et al. (2009) accounted for the effect of surface heave while deducing expressions to quantify the self-weight induced bearing capacity factors under vertical and horizontal loads. These self-weight factors could be used to estimate corresponding f_b values. Nevertheless, the expressions were limited to the horizontal and vertical movements only and this research considered soil with uniform shear strength s_u for their analyses. Chatterjee (2012) has also carried out small strain and LDFE analyses to study the superposing effect of soil self-weight and surface heave on the mobilized horizontal resistance for pipe movement in different directions. Chatterjee et al. (2012b) estimated f_b factor for soil (during mobilization of vertical capacity) with linearly varying shear strength profile. A relationship between f_b and a nondimensional strength parameter involving submerged unit weight γ' and s_u was reported. Chatterjee et al. (2014) proposed separate buoyancy factors for the vertical and horizontal component of the breakout resistance (i.e., f_{bv} and f_{bh}). Although, the study was limited to small strain analyses and did not consider the effect of surface heave. Also, this study was limited to proposing f_{bv} and f_{bh} for uniform shear strength of the soil and pure vertical and horizontal movement of the pipe.

The direction of the pipe movement during lateral buckling is dependent on its weight relative to the strength of the surrounding soil (Chatterjee et al. 2012a). Therefore, the estimation of lateral breakout capacity is not limited to only the vertical and horizontal directions, rather involves calculation of mobilized soil resistance against pipe movement for the complete spectrum of the inclined directions. Consequently, it was realized that the estimation of f_b is dependent on the direction of pipe movement, along with the soil weight and surface heave due to its inherent association with the mobilized soil volume (Merifield et al. 2009; Chatterjee 2012). It is also important to assess how the buoyancy factors for different directions of pipe movement vary with the shear strength profile of the soil. To the best of the authors' knowledge, such a generalized framework to estimate the buoyancy factors for pipe movement in various inclinations is yet to be reported.

This paper investigates the influence of surface heave on the buoyancy component of breakout resistance of pipes moving in different directions. A series of large deformation finite element analyses were performed to capture the heave

formation during pipe penetration (to simulate the pipe installation process) in soft clays. In these analyses, soil with different linearly varying shear strength profiles were considered. After embedding the pipe to the desired depth, the pipe was displaced in different directions till failure. Obtained results are used to analyze the resistance component induced by soil weight and further to compute the buoyancy factors for different directions of pipe movement. The findings from this study can be useful for the precise and efficient design of on-bottom pipelines against lateral breakout capacity.

2 LARGE DEFORMATION FINITE ELEMENT MODEL

2.1 *RITSS approach*

Using commercial finite element (FE) software ABAQUS (Dassault Systèmes, 2023), two-dimensional plane strain FE analyses were performed. The pipe was considered as a weightless rigid body where it was gradually pushed (in a displacement-controlled approach) into the deformable soil from the ground surface. Such a procedure simulates the pipe installation and its consequence on the surrounding ground conditions. The large deformation finite element (LDFE) analyses employed for this study is based on the 'Remeshing and Interpolation Technique with Small Strain' (RITSS; Hu and Randolph

1998a, 1998b). The fundamental reason behind selecting such a technique is in its capability to capture the progressive formation of the surface heave (without inducing any form of element distortion) and the simultaneous interpolation of the material stresses to the modified geometry as the pipe reaches to its desired embedment w.

The RITSS analysis divided the complete pipe penetration process in a series of small strain analyses where 1% of pipe diameter (D) was applied as the incremental displacement in vertically downward direction for each step. The deformed regime after each small strain analysis was re-discretized and consequently, stress, strain and relevant material properties were interpolated from old mesh to new mesh. The re-discretized geometry and material properties mapped to the new nodal coordinates at the end of a step was subsequently used as the initial conditions for the immediate next step. The whole numerical analysis was executed using ABAQUS with the model development (remeshing), post-processing of the results, mapping of variables was performed using Python and FORTRAN programming languages.

2.2 *Problem geometry and material properties*

Figure 1 illustrates a typical representation of the discretized domain at the start of the analyses where the pipe (diameter D = 1m) is placed at the surface of a saturated clay bed. The boundaries of the model are extended 5 times the diameter in lateral (in either direction from the invert of the pipe) and vertical directions. These dimensions are found to be remote enough not to induce any boundary constraint on the results. Both the pipe and the soil are modelled using 6 noded quadratic plane strain triangular elements (CPE6 of ABAQUS standard library). The lateral boundaries were restrained in horizontal direction whereas the bottom boundary was restrained in both horizontal and vertical directions. The pipe-soil interface considered as frictionless and the separation at the pipe-soil interface was allowed under infinitesimal tensile normal stress.

The soil was considered weightless as well as with a submerged unit weight (γ') in the separate sets of analyses. The purpose of conducting analyses with and without considering the soil weight is to estimate the effect of soil buoyancy on the induced lateral breakout resistance. The soil was modelled using perfectly plastic 'Tresca' soil constitutive model where the undrained shear strength of the soil was varied linearly along the depth (i.e., $s_{uz}=s_{um}+k*z$; where s_{uz} and s_{um} are the undrained shear strength of soil at depth z and mudline respectively, k is the gradient of the shear strength profile). The s_{um} is kept as 1 kPa and k was considered as 1, 4 and 10 kPa/m. Accordingly, the non-dimensional strength parameter kD/s_{um} for the analyses was equal to 1, 4, 10. The purpose of this exercise was to investigate the influence of different shear strength profiles on the mobilized buoyant resistance. For these analyses, submerged weight of the soil γ' is considered as 6 kN/m^3 (which makes another non-dimensional parameter, soil weight to strength ratio $\gamma'D/s_{um}$ = 6). In a separate set of analyses, $\gamma'D/s_{um}$ was varied as 4, 8 and 10 keeping the kD/s_{um} = 1 (i.e., γ' = 4, 6 and 10). Young's modulus and Poisson's ratio for the soil were considered as 500*s_u and 0.495, respectively.

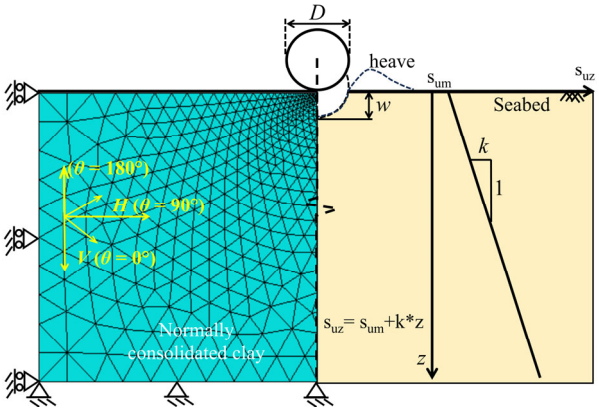

Figure 1. Schematic diagram of the problem (right) and typical mesh with boundary condition (left) and loading directions

Following the RITSS approach, the pipe was penetrated up to half of its diameter (i.e., the normalized vertical embedment w/D was increased up to 0.5). After the completion of the LDFE analysis (as the pipe reached its desired embedment), the pipe was displaced in different inclinations with respect to the vertical axis (to simulate the pipe movement during its breakout). The displacement was applied at the invert of the pipe (defined as a rigid body). For the present study, the pipe was displaced in 13 different directions starting from 0 (i.e., vertically downward) to 180 degrees (i.e., vertically upward) with probe angle is varying by 15 degrees.

3 RESULTS AND DISCUSSION

3.1 *Formation of soil heave*

Performing large deformation finite element analyses aided in capturing the progressively growing soil heave surrounding the pipe, as it moves to a greater embedment. Figure 2 demonstrates a typical heave formation at the ground surface when the pipe gains an embedment equal to half of its diameter. This figure also compares maximum elevation and the lateral spread of the heave formed at the surface for soil with different kD/s_{um} (i.e., for different values strength gradient k). This comparison reveals that the heave is more pronounced as well as concentrated for the soil with higher k value. Consequently, the maximum elevation of the surface heave for kD/s_{um} = 10 is higher, however its width is smaller compared to the surface heave for kD/s_{um} = 1. Such a difference in the dimensions of the heave plays a key role in influencing the lateral breakout resistance, particularly when the embedded pipe is subjected to displacement in different inclinations. Merifield et al. (2009) reported that different dimensions of the heave become predominant while estimating the buoyant resistance against

pipe movement in different directions (i.e., maximum elevation plays a dominating role for horizontal capacity and total heave width becomes predominant for vertical capacity). Furthermore, the higher elevation of the heave causes a higher change in the potential energy, which eventually increases the soil weight component within the mobilized resistance (for both the capacities). The latter component (i.e., the increment in the work done to make higher alteration in the potential energy) contributes significantly in the increase in buoyancy factors with the increase in kD/s_{um} values. The elevation of the heave also influences the pipe's exposure to hydrodynamic loading from waves and current as well as it regulates the thermal losses along the pipeline by controlling the local embedment (i.e., the sum of heave height and embedment) [Chatterjee 2012]. The present research does not attempt to establish a direct correlation between the heave dimensions with the buoyancy factors, however, aims to understand their effect on the estimated f_b values for different directions of pipe movement. The effect of kD/s_{um} on the dimension of the induced heave also resonates with the findings from Chatterjee et al. (2012b) where the buoyancy effect was found to increase with the increase in the non-dimensional soil strength parameter.

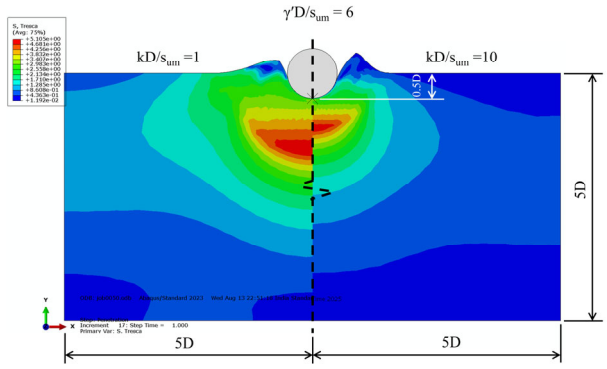

Figure 2. Heave formation at the ground surface during pipe embedment equal to 0.5D in soil with kD/s_{um} = 1 (left) and 10 (right)

3.2 *Estimation of the buoyancy f_b factor*

Parallel sets of LDFE analyses were performed with and without considering self-weight of the soil to quantify the contribution of the buoyant resistance within the total mobilized resistance. Figure 3 compares the normalized vertical capacities ($V/Ds_{u,inv}$; where $s_{u,inv}$ is the shear strength at the pipe invert) for weightless and weighty conditions in soil with kD/s_{um} = 1, 4 and 10. While demonstrating normalized vertical capacities at different normalized embedment (Fig. 3a) $s_{u,inv}$ represents the shear strength at that specific embedment. Whereas while normalizing breakout capacities (Fig. 3b), $s_{u,inv}$ is kept as shear strength at 0.5D embedment. Adoption of $s_{u,inv}$ as the shear strength to normalize the capacities is appropriate in case of an embedded pipe as the failure mechanism extends in either direction from the pipe invert (Merifield et al. 2008; Dingle et al. 2008). Figure 3a demonstrates progressive growth of the soil resistance for the pipe with increasing embedment. The mobilized resistance in weightless condition provides an estimation of the shear resistance. Accordingly, the difference between the total resistances obtained from weighty and weightless conditions provides a direct estimate of the buoyant resistance. The same relationship is demonstrated in the Equation 1a. As discussed, s_u is considered as $s_{u,inv}$ in Eq. 1. Note that, this calculation process assumes that the penetration mechanism, i.e., the geotechnical resistance component remains unaffected with the introduction of the soil self-weight (Chatterjee et al. 2012b). This assumption seems appropriate for the present research (predominantly focused on calculating f_b factors for pipe embedment of 0.5D) as the normalized contact length between pipe and soil remains unchanged even with the development of surface heave for pipe embedment of 0.5D (Merifield et al. 2009). The computation of vertical buoyancy factors f_{bv} with the pipe embedment shows a considerable increase with the increase in the kD/s_{um} values (Fig. 4). In the expression shown in Equation 1, A_s is the embedded pipe area, γ' is the submerged unit weight and D is the pipe diameter. The embedded pipe area continuously grows with the increase in embedment and consequently calculated using the expression given in Chatterjee et al. (2014). Therefore, $\gamma' A_s$ is the weight of the displaced soil by the pipe.

As discussed in Section 2, after embedding the pipe with RITSS approach to w/D = 0.5, the same pipe was displaced in an array of different directions. The resistance offered by the weightless and weighty soil with kD/s_{um} = 1, 4 and 10 against pipe movement in different directions is illustrated in Fig. 3b. Introduction of the soil weight induces a variation in the mobilized capacities, however, upon estimation of buoyancy factors using Equation 1, f_{bv} and f_{bh} (vertical and horizontal buoyancy factors respectively) varies within a small range for different kD/s_{um}. Note that, the vertical and horizontal capacities were normalized with the undrained shear strength at the invert of the pipe, $s_{u,inv}$ (Fig. 3b). As discussed before, for normalizing all the capacities, the s_u at the invert of the pipe has been used. As the small strain analyses are performed at a particular embedment (i.e., 0.5D) to compute the breakout capacities, consideration of $s_{u,inv}$ as the representative s_u value deemed appropriate for Fig. 3b (Randolph and White 2008; Merifield et al. 2009).

The expression presented in Equation 1 to compute f_{bv} and f_{bh} (adopted from Chatterjee et al. 2014) was primarily developed to estimate the buoyancy factors for wished-in-place pipes. Preliminary verification of these expressions was conducted through comparison of the obtained f_b factors (for a wished-in-place pipe) with the reported values from literature. The factor f_{bv} was estimated to be 1.0 and 0.5 for vertical and horizontal pipe movements respectively, whereas f_{bh}~0.3 for horizontal movement. Nonetheless, the same expressions are used in the present research to provide refined f_b factors that includes the effect of surface heave in clays with different shear strength profiles.

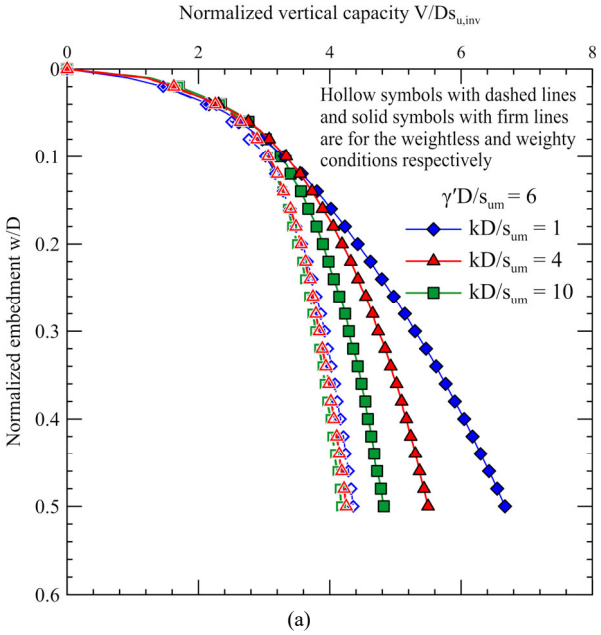

(a)

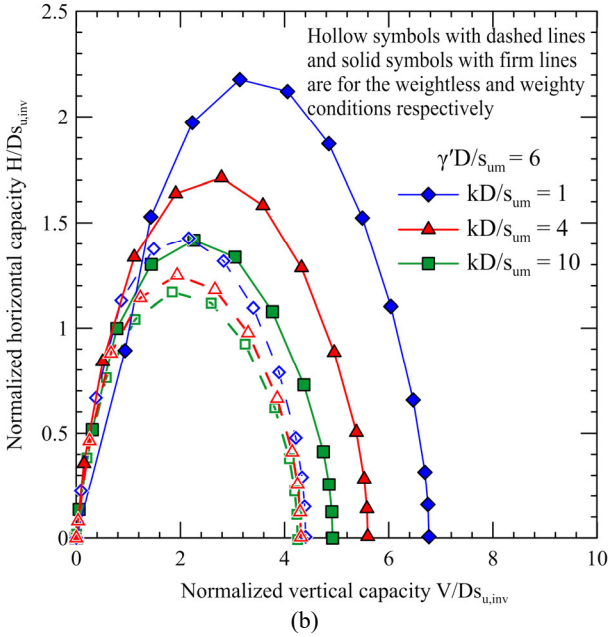

Figure 3. Comparison of the (a) normalized vertical capacities with normalized embedment and (b) normalized vertical and horizontal capacities at w/D = 0.5 for weightless and weighty condition ($\gamma'D/s_{um}$ = 6) in soil with kD/s_{um} = 1, 4 and 10

$$\left(\frac{V}{Ds_u}\right)_{weighty} = \left(\frac{V}{Ds_u}\right)_{weightless} + f_{bv}\frac{\gamma' A_s}{Ds_u} \quad (1a)$$

$$\left(\frac{H}{Ds_u}\right)_{weighty} = \left(\frac{H}{Ds_u}\right)_{weightless} + f_{bh}\frac{\gamma' A_s}{Ds_u} \quad (1b)$$

3.3 *Influence of shear strength gradient and unit weight of soil on f_b*

Figure 4a demonstrates the variation of the vertical buoyancy factor f_{bv} along the embedment for kD/s_{um} = 1, 4 and 10 (with the colored plots). For these plots, nondimensional parameter $\gamma'D/s_{um}$ has been kept as 6. This comparison shows that the f_{bv} remains nearly constant with the depth of embedment. However, f_{bv} attains different values consistently across the considered range of embedment with the variation in kD/s_{um} values. This variation is due to the difference in the maximum elevation and lateral spread of the induced heave (as shown in Fig. 2). The obtained f_{bv} values in soil with different shear strength profiles are also compared with the linear relationship between f_{bv} and $kD/s_{u,avg}$ proposed in Chatterjee et al. (2012b). Here, $s_{u,avg}$ is the average shear strength for a depth extending from the mudline to one diameter of pipe. Figure 4b shows that the f_{bv} factors calculated using the expression proposed by Chatterjee et al. (2012b) and those estimated from the present study are in complete agreement with each other.

The effect of another nondimensional parameter $\gamma'D/s_{um}$ has also been studied. The shear strength profile of the soil has been kept unchanged in these analyses and only γ' was varied. Here, the shear strength parameter kD/s_{um} is kept as 1 and the values of $\gamma'D/s_{um}$ are taken as 4, 6, 8 and 10. Figure 4a also demonstrates the f_{bv} values in soil with varying $\gamma'D/s_{um}$ (in grey scale plots). The factor f_{bv} is found to slightly decrease (across the range of embedment) with the increase in γ', however, this decrease is very small. It was also observed from the resulting contour plots from the analyses involving different γ' that the heave profile undergoes negligible alteration with the change in soil weight. Therefore, the buoyancy factors can be considered to remain almost unaffected with the change in γ', such an observation echoes with findings reported in Chatterjee et al. (2012b).

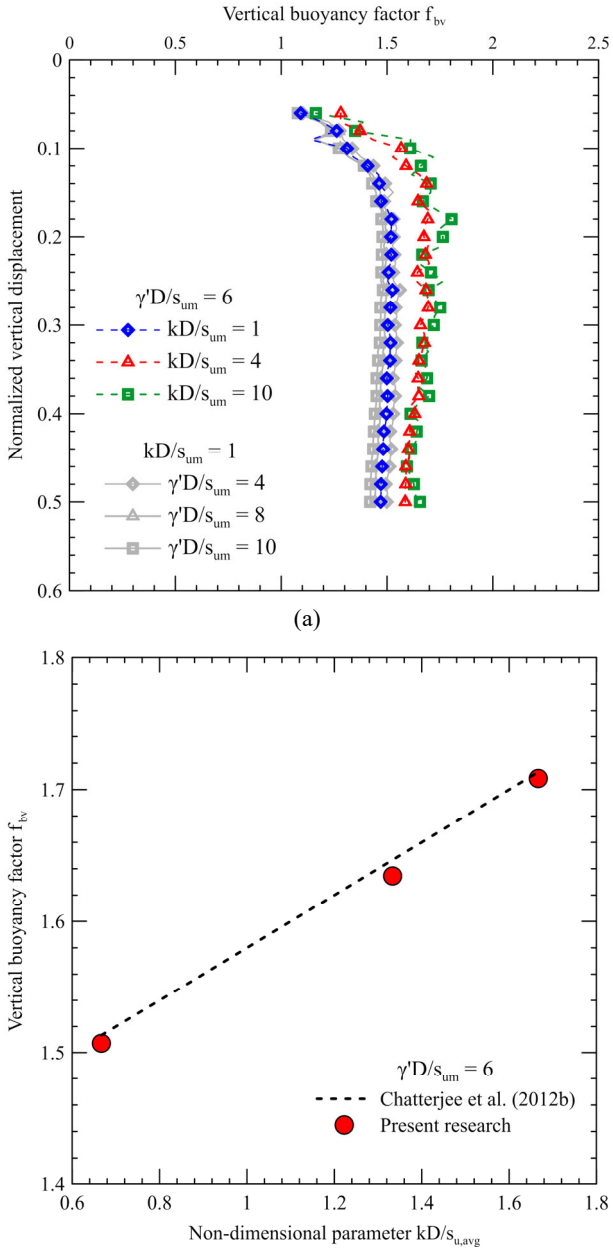

Figure 4. Variation of the vertical buoyancy factor with normalized embedment; (a) comparison of the f_{bv} values for soil with $\gamma'D/s_{um}$ = 6, kD/s_{um} = 1, 4 and 10 (shown in color) and $\gamma'D/s_{um}$ = 4, 8 and 10, kD/s_{um} = 1 (shown in grey scale) (b) comparison between the obtained f_{bv} and the predicted values using the expression reported in Chatterjee et al. (2012b)

The evolution of vertical and horizontal buoyancy factors (f_{bv} and f_{bh}) for soil with different strength gradients and submerged unit weight was also studied through performing small strain analyses at w/D = 0.5. Figure 5 demonstrates the variation of these factors with the probe angle (calculated as the angle between the direction of pipe movement and vertical downward direction). The f_{bv} factor for higher k is found to be higher particularly when the probe angle is small (Fig. 4a). For higher probe angle, this trend reverses. Whereas the horizontal buoyancy factor f_{bh} is found to be consistently higher for the greater k value (Fig. 5b).

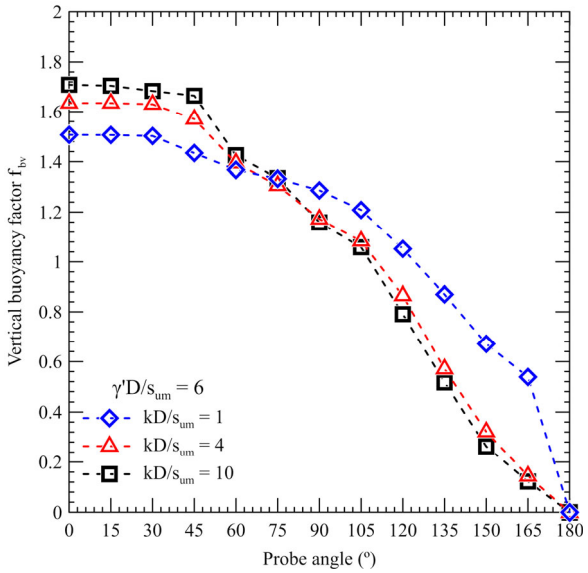

(a)

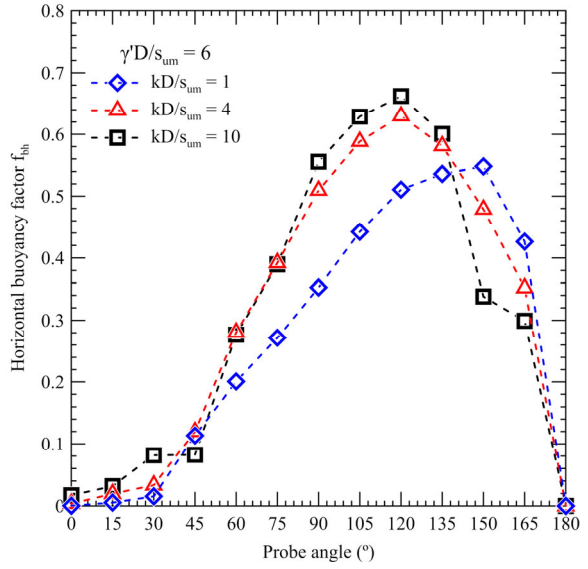

(b)

Figure 5. Variation of vertical (f_{bv}) and horizontal (f_{bh}) buoyancy factors with probe angle for kD/s_{um} = 1, 4 and 10

Table 1 reports the f_{bv} and f_{bh} factors estimated during inclined breakout of on bottom pipelines for soil with different strength gradients. The table shows that the value of f_{bv} for kD/s_{um} = 1 is found to be 1.5 (for vertical pipe movement, i.e., probe angle 0°, at w/D =0.5). This value agrees with the value reported in Merifield et al. (2009). Nevertheless, the f_{bv} increases to 1.635 and 1.708 for kD/s_{um} = 4 and 10 respectively. This f_{bv} value for kD/s_{um} = 7 was computed as 1.670. Therefore, it can be observed that the increase in f_{bv} with kD/s_{um} gradually reduces as kD/s_{um} attains a higher value. Such a trend matches with the f_{bv} value (=1.75) reported for kD/s_{um} = 20 in Chatterjee et al. (2012b). The f_{bv} during horizontal movement (i.e., probe angle 90°) is found to be 0.5 with wished in place pipe in uniform soil, kD/s_{um} = 0 (Merifield et al. 2009). Precise consideration of the heave increases the same f_{bv} for kD/s_{um} = 1 to 1.287. Moreover, the f_{bh} for horizontal movement was estimated as $(0.5*w^2)/A_s$ analytically. The same f_{bh} is found as 0.353 for kD/s_{um} = 1 and higher for higher kD/s_{um} values. This also shows the direct effect of the formed surface heave on the buoyancy factor. Overall, such a table could be very useful while designing the pipeline against lateral breakout in soft clays.

4 CONCLUSIONS

The present research performed large deformation finite element analyses considering soil with and without self-weight, particularly to quantify the resistance induced by soil weight (also referred as buoyant resistance) during inclined lateral breakout of on-bottom pipelines in clay. The LDFE analyses are performed to capture the non-linearities associated with the problem geometry (i.e., heave formation). At the end of LDFE analysis, when the pipe gains its desired embedment of half a diameter considered here, the same pipe was subjected to various combinations of vertical and horizontal displacements to failure. Accounting for the effect of heave formation on the induced lateral breakout resistance helps in precise estimation of the buoyancy factors. An expression already available in the literature was used to provide a refined set of buoyancy factors for vertical and horizontal capacities (i.e., f_{bv} and f_{bh}), considering the effect of heave, for soil with different shear strength gradients and soil weight to strength ratios. The surface heave formation is found to be significantly influenced by the shear strength gradient of the soil and consequently, the shear strength gradient influences the estimated buoyancy factors for inclined lateral breakout of a pipeline. The submerged unit weight of the soil was found to have minimum influence on the buoyant resistance. Finally, the buoyancy factors for a range of soil strength profiles are provided in a tabulated manner. This table can be useful for the readers/practitioners while estimating inclined lateral breakout resistance of pipelines in normally consolidated clay.

Table 1. Buoyancy factors f_{bv}, f_{bh} against inclined breakout for kD/s_{um} = 1, 4, 10 (γ'D/s_{um} = 6)

Probe Angle ( )	kD/s_{um} = 1		kD/s_{um} = 4		kD/s_{um} = 10	
	f_{bv}	f_{bh}	f_{bv}	f_{bh}	f_{bv}	f_{bh}
0	1.507	0.000	1.635	0.004	1.708	0.017
15	1.506	0.005	1.634	0.019	1.705	0.032
30	1.503	0.015	1.630	0.033	1.683	0.081
45	1.434	0.113	1.570	0.120	1.664	0.082
60	1.368	0.201	1.395	0.281	1.425	0.277
75	1.333	0.272	1.306	0.392	1.334	0.390
90	1.287	0.353	1.173	0.510	1.159	0.556
105	1.209	0.442	1.083	0.588	1.058	0.629
120	1.052	0.511	0.865	0.630	0.790	0.662
135	0.870	0.536	0.571	0.581	0.517	0.601
150	0.671	0.548	0.321	0.479	0.263	0.338
165	0.538	0.426	0.144	0.352	0.122	0.299
180	0.000	0.000	0.000	0.000	0.000	0.000

5 REFERENCES

Bruton, D. A. S., White, D. J., Cheuk, C. Y., Bolton, M. D. and Carr, M. C. 2006. Pipe–soil interaction behaviour during lateral buckling, including large amplitude cyclic displacement tests by the Safebuck JIP. *Proc. Offshore Technology Conference, Houston,* OTC 17944.

Chatterjee, S. 2012. Numerical modelling of pipe-soil interactions, University of Western Australia.

Chatterjee, S., White, D. J. and Randolph, M. F. 2012a. Numerical simulations of pipe–soil interaction during large lateral movements on clay. *Géotechnique*, 62(8), 693–705.

Chatterjee, S., Randolph, M. F., and White, D. J. 2012b. The effects of penetration rate and strain softening on the vertical penetration resistance of seabed pipelines. *Géotechnique*, 62(7), 573-582.

Chatterjee, S., Gourvenec, S., and White, D. J. 2014. Assessment of the consolidated breakout response of partially embedded subsea pipelines. *Géotechnique*, 64(5), 391-399.

Dassault Systemes, 2023. Abaqus User's Manual, Version 6.23.

Dingle, H. R. C., White, D. J. & Gaudin, C. 2008. Mechanisms of pipe embedment and lateral breakout on soft clay. Canadian Geotechnical Journal 45(5), 636–652

Hu, Y., and Randolph, M. F. 1998a. A practical numerical approach for large deformation problems in soil. *International Journal Numerical and Analytical Methods in Geomechanics*, 22(5), 327–350.

Hu, Y., and Randolph, M. F. 1998b. H-adaptive FE analysis of elastoplastic non-homogeneous soil with large deformation. Computers and Geotechnics, 23(1–2), 61–83.

Merifield, R., White, D. J., and Randolph, M. F. 2008. The ultimate undrained resistance of partially embedded pipelines. *Géotechnique*, 58(6), 461-470.

Merifield, R. S., White, D. J. and Randolph, M. F. 2009. Effect of surface heave on response of partially embedded pipelines on clay. *Journal of Geotechnical and Geoenvironmental Engineering*, ASCE 135(6), 819– 829.

Randolph, M. F., and White, D. J. 2008. Pipeline embedment in deep water: process and quantitative assessment. *Proc. of the Offshore Technology Conference, Houston,* OTC 19128.

White, D. J., and Cathie, D. N. 2011. Geotechnics for subsea pipelines. *Frontiers in offshore geotechnics II*, *1*, 87-123.